

# On Occupation Kernels, Liouville Operators, and Dynamic Mode Decomposition

Joel A. Rosenfeld<sup>1</sup>, Rushikesh Kamalapurkar<sup>2</sup>, L. Forest Gruss<sup>3</sup>, and Taylor T. Johnson<sup>4</sup>

**Abstract**—Using the newly introduced “occupation kernels,” the present manuscript develops an approach to dynamic mode decomposition (DMD) that treats continuous time dynamics, without discretization, through the Liouville operator. The technical and theoretical differences between Koopman based DMD for discrete time systems and Liouville based DMD for continuous time systems are highlighted, which includes an examination of these operators over several reproducing kernel Hilbert spaces.

## I. INTRODUCTION

Dynamic mode decomposition (DMD) has emerged as an effective method of extracting fundamental governing principles from high-dimensional time series data. The method has been employed successfully in the field of fluid dynamics, where DMD methods have demonstrated an ability to determine dynamic modes, also known as “Koopman modes,” which agree with Proper Orthogonal Decomposition (POD) analyses (cf. [1–7]). However, DMD methods employing Koopman operators do not address continuous time dynamical systems directly. Instead, current DMD methods analyze discrete time proxies of continuous time systems [3]. The discretization process constrains Koopman based DMD methods to systems that are forward complete [8]. The objective of the present manuscript is to develop DMD methods that avoid discretization of continuous time dynamical systems, while providing convergence results that are stronger than Koopman based DMD and applicable to a broader class of dynamical systems.

For example, discretization of the continuous time dynamical system  $\dot{x} = 1 + x^2$  with time step 1 yields the following discrete dynamics:  $x_{i+1} = F(x_i) := \tan(1 + \arctan(x_i))$ . It should be immediately apparent that  $F$  is not well defined over  $\mathbb{R}$ . In fact, through the consideration of  $x_i = \tan(\pi/2 - 1)$  it can be seen that  $F(x_i)$  is undefined. Since the symbol for a Koopman operator must be defined over the entire domain, there is no well defined Koopman operator arising from this discretization. Hence, the resultant

Koopman operator cannot be expected to be well-defined. Note that the example above is not anecdotal. In addition to commonly used examples in classical works, such as [9], mass-action kinetics in thermodynamics [10, Section 6.3], chemical reactions [11, Section 8.4], and species populations [12, Section 4.2] often give rise to such models. In general, unless the solutions of the continuous time dynamics are constrained to be forward complete, (for example, by assuming that the dynamical systems are globally Lipschitz [13, Chapter 1]) the resultant Koopman operator cannot be expected to be well-defined. This observation is validated by [8], but otherwise conditions on the dynamics are largely absent from the literature.

Even in the case of globally Lipschitz models, results regarding convergence of the DMD operator to the Koopman operator rely on the assumption that the Koopman operator is bounded over a specified RKHS (cf. [14]). Boundedness of composition operators, like the Koopman operator, has been an active area of study in the operator theory community. Indeed, it turns out there are very few bounded composition operators over many function spaces. A canonical example is in the study of the Bargmann-Fock space, where only affine symbols yield bounded composition operators and of those the compact operators arise from  $F(z) = az + b$  where  $|a| < 1$ . This is a very small collection, and reveals how unlikely it is to have a bounded Koopman operator arising from the discretization of continuous time nonlinear systems.

A subset of Liouville operators that require the assumption of forward completeness on the dynamical system, called Koopman generators, have been studied as limits of Koopman operators in works such as [15–20]. The present work sidesteps the limiting process, and as a result, the assumptions regarding existence of Koopman operators, through the use of “occupation kernels”. Specifically, occupation kernels remove the burden of approximation from that of operators and places it on the estimation of occupation kernels from time-series data, which requires much less theoretical overhead. The action of the adjoint of a Liouville operator on an occupation kernel provides the input-output relationships that enable DMD of time series data. Consequently, Liouville operators may be directly examined via occupation kernels, while avoiding limiting relations involving Koopman operators that might not be well defined for a particular discretization of a continuous time nonlinear dynamical system.

The direct involvement of Liouville operators in a DMD routine allows for the study of dynamics that are locally rather than globally Lipschitz, since Liouville operators do

\*This research was supported, in part, by the Air Force Office of Scientific Research under award number FA9550-20-1-0127, FA9550-15-1-0258, FA9550-16-1-0246, and FA9550-18-1-0122, the Air Force Research Laboratory under contract number FA8651-19-2-0009, the Office of Naval Research under contract N00014-18-1-2184, and the National Science Foundation under award number 2027999. Any opinions, findings, or recommendations in this article are those of the author(s), and do not necessarily reflect the views of the sponsoring agencies.

<sup>1</sup> University of South Florida, email: joelr@usf.edu.

<sup>2</sup> Oklahoma State University, email: rushikesh.kamalapurkar@okstate.edu.

<sup>3</sup> University of South Florida, email: lgrussrosenfeld@usf.edu.

<sup>4</sup> Vanderbilt University, email: taylor.johnson@vanderbilt.edu.

not impose an *a priori* discretization. For the adjoint of a Liouville operator to be well defined, the operator must be densely defined over the underlying RKHS [21, 22]. As a result, the exact class of dynamical systems that may be studied using Liouville operators depends on the selection of the RKHS. However, the requirement that the Liouville operator must be densely defined is not overly restrictive. For example, on the real valued Bargmann-Fock space, Liouville operators are densely defined for a wide range of dynamics that are expressible as real entire functions (which includes polynomials, exponential functions, sine, and cosine functions, etc.).

The relevant preliminary concepts for the theoretical underpinnings of the approach taken in the present manuscript are reviewed in Section II-A. This includes definitions and properties of RKHSs as well as densely defined operators and their adjoints.

## II. TECHNICAL PRELIMINARIES

### A. Reproducing Kernel Hilbert Spaces

**Definition 1.** A reproducing kernel Hilbert space (RKHS) over a set  $X$  is a Hilbert space of functions from  $X$  to  $\mathbb{R}$  such that for each  $x \in X$ , the evaluation functional  $E_x g := g(x)$  is bounded.

By the Reisz representation theorem, corresponding to each  $x \in X$  there is a function  $k_x \in H$  such that for all  $g \in H$ ,  $\langle g, k_x \rangle_H = g(x)$ . The kernel function corresponding to  $H$  is given as  $K(x, y) = \langle k_y, k_x \rangle_H$ . The kernel function is a positive definite function in the sense that for any finite number of points  $\{c_1, c_2, \dots, c_M\} \subset X$ , the corresponding Gram matrix is positive semi-definite.

### B. Adjoints of Densely Defined Liouville Operators

Unbounded operators over a Hilbert space are linear operators given as  $W : \mathcal{D}(W) \rightarrow H$ , where  $\mathcal{D}(W)$  is the domain contained within  $H$  on which the operator  $W$  is defined [23, Chapter 5]. When the domain of  $W$  is dense in  $H$ ,  $W$  is said to be a densely defined operator over  $H$ . While unbounded operators are by definition discontinuous, closed operators over a Hilbert space satisfy weaker limiting relations. That is, an operator is closed if  $\{g_m\}_{m=1}^\infty \in \mathcal{D}(W)$ , and both  $\{g_m\}_{m=1}^\infty$  and  $\{Wg_m\}_{m=1}^\infty$  are convergent sequences where  $g_m \rightarrow g \in H$  and  $Wg_m \rightarrow h \in H$ , then  $g \in \mathcal{D}(W)$  and  $Wg = h$  [23, Chapter 5]. The Closed Graph Theorem states that if  $W$  is a closed operator such that  $\mathcal{D}(W) = H$ , then  $W$  is bounded.

**Lemma 2.** A Liouville Operator with symbol  $f$  that has the canonical domain

$$\mathcal{D}(A_f) := \{g \in H : \nabla g \cdot f \in H\},$$

is closed over RKHSs that are composed of continuously differentiable functions.

*Proof.* See [22].  $\square$

The closedness of Koopman operators is well known in the study of RKHS, where they are more commonly known

as composition operators (cf. [24, 25]). Beyond the limit relations provided by closed operators, the closedness of an unbounded operator plays a significant role in the study of the adjoints of unbounded operators [23, Chapter 5].

**Definition 3.** For an operator  $W$  let

$$\mathcal{D}(W^*) := \{h \in H : g \mapsto \langle Wg, h \rangle_H \text{ is bounded} \}$$

be dense in  $H$ . For each  $h \in \mathcal{D}(W^*)$  the Reisz theorem guarantees a function  $W^*h \in H$  such that  $\langle Wg, h \rangle_H = \langle g, W^*h \rangle_H$ . The adjoint of the operator  $W$  is thus given as  $W^* : \mathcal{D}(W^*) \rightarrow H$  via the assignment  $h \mapsto W^*h$ .

For a closed operator over a Hilbert space, the adjoint is densely defined [23]. Hence, Liouville operators with domains given as in Lemma 2, their adjoints are densely defined. To characterize the interaction between the trajectories of a dynamical system and the Liouville operator, the notion of occupation kernels must be introduced (cf. [22]).

**Definition 4.** Let  $X$  be a metric space,  $\gamma : [0, T] \rightarrow X$  be an essentially bounded measurable trajectory, and let  $H$  be a RKHS over  $X$  consisting of continuous functions. Then the functional  $g \mapsto \int_0^T g(\gamma(t))dt$  is bounded, and the Reisz theorem guarantees a function  $\Gamma_\gamma \in H$  such that

$$\langle g, \Gamma_\gamma \rangle_H = \int_0^T g(\gamma(t))dt$$

for all  $g \in H$ . The function  $\Gamma_\gamma$  is the *occupation kernel* corresponding to  $\gamma$  in  $H$ .

**Lemma 5.** Let  $f : \mathbb{R}^n \rightarrow \mathbb{R}^n$  be the dynamics for a dynamical system, and suppose that  $\gamma : [0, T] \rightarrow \mathbb{R}^n$  is a trajectory satisfying  $\dot{\gamma} = f(\gamma(t))$  in the Caratheodory sense. In this setting,  $\Gamma_\gamma \in \mathcal{D}(A_f^*)$ . Moreover,  $A_f^* \Gamma_\gamma = K(\cdot, \gamma(T)) - K(\cdot, \gamma(0))$ .

*Proof.* See [22].  $\square$

## III. OCCUPATION KERNEL DYNAMIC MODE DECOMPOSITION

With the relevant theoretical background presented, this section develops the Occupation Kernel-based DMD method for continuous time systems. This method differs from the kernel-based extended DMD method of [7], where the kernel functions for the inputs are now replaced by occupation kernels, and the output is now a difference of kernel functions. This formulation allows for the snapshots of typical DMD methods to be strung together as trajectories. The occupation kernel-based DMD method then allows for the incorporation of all the snapshots of a given system to be incorporated into the DMD analysis in a way that reduces the dimensionality of the resultant problem to be less than the number of snapshots, while simultaneously allowing for the direct treatment of continuous time dynamical systems. If the rank of the resulting matrices needs to be increased, the trajectories may be segmented up to the number of snapshots.

It should also be noted that this method differs from [7] in that it avoids direct evaluations of the feature space. Thus, the

succeeding method keeps with the spirit of the “kernel trick,” where the feature space is only accessed through evaluation of the kernel functions [26, pg. 19].

Let  $K$  be the kernel function for a RKHS,  $H$ , over  $\mathbb{R}^n$  consisting of continuously differentiable functions. Let  $\dot{x} = f(x)$  be a dynamical system corresponding to a densely defined Liouville operator,  $A_f$ , over  $H$ . Suppose that  $\{\gamma_i : [0, T_i] \rightarrow X\}_{i=1}^M$  is a collection of trajectories satisfying  $\dot{\gamma}_i = f(\gamma_i)$ . There is a corresponding collection of *occupation kernels*,  $\alpha := \{\Gamma_{\gamma_i}\}_{i=1}^M \subset H$ , given as  $\Gamma_{\gamma_i}(x) := \int_0^{T_i} K(x, \gamma_i(t)) dt$ . For each  $\gamma_i$  the action of  $A_f^*$  on the corresponding occupation kernel is  $A_f^* \Gamma_{\gamma_i} = K(\cdot, \gamma_i(T_i)) - K(\cdot, \gamma_i(0))$ .

Thus, when  $\alpha$  is selected as an ordered basis for a vector space, the action of  $A_f^*$  is known on  $\text{span}(\alpha)$ . The objective of the DMD procedure is to express a matrix representation of the operator  $A_f^*$  on the finite dimensional vector space spanned by  $\alpha$  followed by projection onto  $\text{span}(\alpha)$ .

Let  $w_1, \dots, w_M$  be the coefficients for the projection of a function  $g \in H$  onto  $\text{span}(\alpha) \subset H$ , written as  $P_\alpha g = \sum_{i=1}^M w_i \Gamma_{\gamma_i}$ . The coefficients  $w_1, \dots, w_M$  may be obtained through the solution of the linear system

$$\begin{pmatrix} \langle \Gamma_{\gamma_1}, \Gamma_{\gamma_1} \rangle_H & \cdots & \langle \Gamma_{\gamma_M}, \Gamma_{\gamma_1} \rangle_H \\ \vdots & \ddots & \vdots \\ \langle \Gamma_{\gamma_1}, \Gamma_{\gamma_M} \rangle_H & \cdots & \langle \Gamma_{\gamma_M}, \Gamma_{\gamma_M} \rangle_H \end{pmatrix} \begin{pmatrix} w_1 \\ \vdots \\ w_M \end{pmatrix} = \begin{pmatrix} \langle g, \Gamma_{\gamma_1} \rangle_H \\ \vdots \\ \langle g, \Gamma_{\gamma_M} \rangle_H \end{pmatrix}, \quad (1)$$

where each of the inner products may be expressed as either single or double integrals as  $\langle \Gamma_{\gamma_j}, \Gamma_{\gamma_i} \rangle_H = \int_0^{T_i} \int_0^{T_j} K(\gamma_i(\tau), \gamma_j(t)) dt d\tau$ , and  $\langle g, \Gamma_{\gamma_i} \rangle_H = \int_0^{T_i} g(\gamma_i(t)) dt$ . Furthermore, given  $h = \sum_{i=1}^M v_i \Gamma_{\gamma_i} \in \text{span}(\alpha)$ , then  $A_f^* h \in H$ , and it follows that

$$\begin{aligned} \langle A_f^* h, \Gamma_{\gamma_j} \rangle &= \left\langle \sum_{i=1}^M v_i A_f^* \Gamma_{\gamma_i}, \Gamma_{\gamma_j} \right\rangle_H = \\ &= \left( \left\langle A_f^* \Gamma_{\gamma_1}, \Gamma_{\gamma_j} \right\rangle_H, \dots, \left\langle A_f^* \Gamma_{\gamma_M}, \Gamma_{\gamma_j} \right\rangle_H \right) \begin{pmatrix} v_1 \\ \vdots \\ v_M \end{pmatrix}, \quad (2) \end{aligned}$$

for all  $j = 1, \dots, M$ . Using (1) and (2), the coefficients  $w_1, \dots, w_M$  in the projection of  $A_f^* h$  onto  $\text{span}(\alpha)$  can be expressed as

$$\begin{aligned} \begin{pmatrix} w_1 \\ \vdots \\ w_M \end{pmatrix} &= \begin{pmatrix} \langle \Gamma_{\gamma_1}, \Gamma_{\gamma_1} \rangle_H & \cdots & \langle \Gamma_{\gamma_M}, \Gamma_{\gamma_1} \rangle_H \\ \vdots & \ddots & \vdots \\ \langle \Gamma_{\gamma_1}, \Gamma_{\gamma_M} \rangle_H & \cdots & \langle \Gamma_{\gamma_M}, \Gamma_{\gamma_M} \rangle_H \end{pmatrix}^{-1} \\ &\times \begin{pmatrix} \langle A_f^* \Gamma_{\gamma_1}, \Gamma_{\gamma_1} \rangle_H & \cdots & \langle A_f^* \Gamma_{\gamma_M}, \Gamma_{\gamma_1} \rangle_H \\ \vdots & \ddots & \vdots \\ \langle A_f^* \Gamma_{\gamma_1}, \Gamma_{\gamma_M} \rangle_H & \cdots & \langle A_f^* \Gamma_{\gamma_M}, \Gamma_{\gamma_M} \rangle_H \end{pmatrix} \begin{pmatrix} v_1 \\ \vdots \\ v_M \end{pmatrix}. \end{aligned}$$

Lemma 5 then yields the finite rank representation for  $P_\alpha A_f^*$ ,

restricted to the occupation kernel basis,  $\text{span}(\alpha)$ , as

$$\begin{aligned} [P_\alpha A_f^*]_\alpha^\alpha &= \begin{pmatrix} \langle \Gamma_{\gamma_1}, \Gamma_{\gamma_1} \rangle_H & \cdots & \langle \Gamma_{\gamma_1}, \Gamma_{\gamma_M} \rangle_H \\ \vdots & \ddots & \vdots \\ \langle \Gamma_{\gamma_M}, \Gamma_{\gamma_1} \rangle_H & \cdots & \langle \Gamma_{\gamma_M}, \Gamma_{\gamma_M} \rangle_H \end{pmatrix}^{-1} \\ &\times \begin{pmatrix} K_{1,1} & \cdots & K_{1,M} \\ \vdots & \ddots & \vdots \\ K_{M,1} & \cdots & K_{M,M} \end{pmatrix} \end{aligned}$$

where

$$K_{i,j} := \langle K(\cdot, \gamma_j(T_j)) - K(\cdot, \gamma_j(0)), \Gamma_{\gamma_i} \rangle_H$$

Suppose that  $\lambda_i$  is the eigenvalue corresponding to the eigenvector,  $v_i := (v_{i1}, v_{i2}, \dots, v_{iM})^T$ ,  $i = 1, \dots, M$ , of  $([P_\alpha A_f^*]_\alpha^\alpha)^T$ , the matrix representation of  $(P_\alpha A_f^*)^*$  restricted to  $\text{span}(\alpha)$ . The eigenvector  $v_i$  can be used to construct a normalized eigenfunction of  $(P_\alpha A_f^*)^*$  restricted to  $\text{span}(\alpha)$ , given as  $\varphi_i = \frac{1}{N_i} \sum_{j=1}^M v_{ij} \Gamma_{\gamma_j}$ , where  $N_i := \sqrt{v^T G v}$  and  $G := (\langle \Gamma_{\gamma_i}, \Gamma_{\gamma_j} \rangle_H)_{i,j=1}^M$  is the Gram matrix corresponding to the occupation kernel basis.

The DMD procedure begins by expressing the identity function, also known as the full state observable,  $g_{id}(x) := x \in \mathbb{R}^n$  as a combination of the approximate eigenfunctions of  $A_f$  and *Liouville modes*  $\xi_i \in \mathbb{R}^n$  as  $g_{id}(x) \approx \sum_{i=1}^M \xi_i \varphi_i(x)$ , where

$$\xi_i = (\langle (x)_1, \varphi_i \rangle_H \quad \cdots \quad \langle (x)_n, \varphi_i \rangle_H)^T$$

and  $(x)_j$  is viewed here as the mapping  $x \mapsto x_j$ . In turn, this yields

$$\xi_i = \frac{1}{N_i} \sum_{j=1}^M v_{ij} \int_0^{T_j} \gamma_j(t) dt.$$

Given a trajectory  $x$  satisfying  $\dot{x} = f(x)$ , each eigenfunction of  $A_f$  satisfies  $\dot{\varphi}_i(x(t)) = \lambda_i \varphi_i(x(t))$  and hence,  $\varphi_i(x(t)) = \varphi_i(x(0)) e^{\lambda_i t}$ , and the following data driven model is obtained:

$$x(t) \approx \sum_{i=1}^M \xi_i \varphi_i(x(0)) e^{\lambda_i t}.$$

#### IV. NUMERICAL EXPERIMENTS

This section gives the results two collections of numerical experiments using the methods of the paper. The first surround the problem of flow across a cylinder, which has become a classic example for DMD. This provides a benchmark for comparison of the present method with kernel-based extended DMD. The second experiment performs a decomposition using electroencephalography (EEG) data, which has been sampled at 250 hz over a period of 8 seconds. The high sampling frequency gives a large number of snapshots, which then leads to a high dimensional learning problem when using the snapshots alone. The purpose of

<sup>1</sup>Here the notation  $(P_\alpha A_f^*)^*$  is used in place of  $P_\alpha A_f$  as  $A_f$  is an unbounded operator, and its domain may not include the occupation kernels that form the basis for  $\text{span}(\alpha)$ . This technicality can be overcome when compact scaled Liouville operators are leveraged for DMD analysis (see [27])

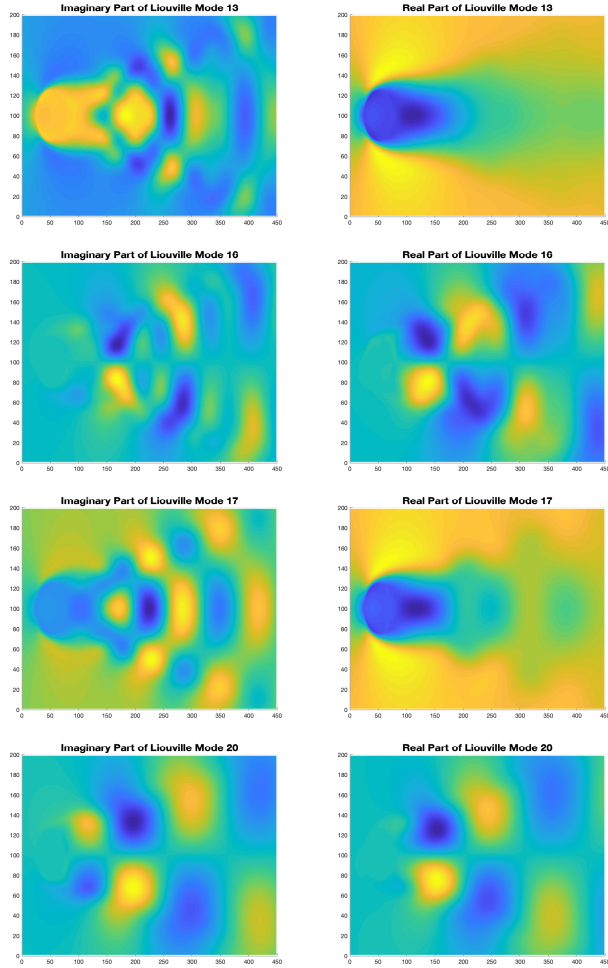


Fig. 1. This figure presents the real and imaginary parts of a selection of ten Liouville modes determined by the continuous time DMD method given in the present manuscript corresponding to the flow across a cylinder data given in [3].

this experiment is to demonstrate how the Liouville operator based DMD can incorporate the large number of snapshots to generate Liouville modes without discarding data.

#### A. Flow Across a Cylinder

This experiment utilizes standard data from [3], which provides a simulation from fluid dynamics. The data corresponds to a wake behind a circular cylinder, and the Reynolds number for this flow is 100. The simulation was generated with time steps of  $\Delta t = 0.02$  second and ultimately sampled every  $10\Delta t$  seconds yielding 150 snapshots. Each snapshot of the system is a vector of dimension 89,351. More details may be found in [3, Chapter 2].

Figure 1 presents the Liouville modes obtained from the cylinder flow data set. The modes were generated using the exponential dot product kernel with  $\mu = 50,000$  and the collection snapshots was subdivided into 50 trajectories of length 3.

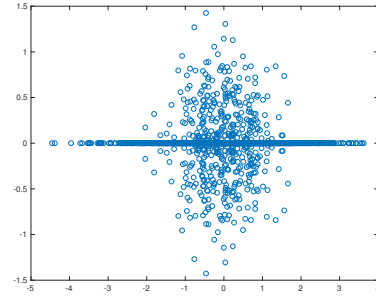


Fig. 2. Eigenvalues corresponding to the ssVEP dataset from [28].

#### B. SsVEP Dataset

This experiment uses data from [28]. The data for this experiment was taken from an electroencephalography (EEG) recording of the visual cortex of one human participant during the active viewing of flickering images [28]. By modulating luminance or contrast of an image at a constant rate (e.g. 12Hz), image flickering reliably evokes the steady state visually evoked potential (ssVEP) in early visual cortex [29, 30], reflecting entrainment of neuronal oscillations at the same driving frequency. SsVEP in the current data was evoked by pattern-reversal Gabor patch flickering at 12Hz (i.e. contrast-modulated) for a trial length of 7 seconds, with greatest signal strength originating from the occipital pole (Oz) of a 129-electrode cap. Data was sampled at 500Hz, band-pass filtered online from 0.5–48Hz, offline from 3–40Hz, with 53 trials retained for this individual after artifact rejection. Of these trials, the first 40 trials were used in the continuous time DMD method and each trial was subdivided into 50 trajectories. SsVEP data have the advantage of having an exceedingly high signal-to-noise ratio and high phase coherence due to the oscillatory nature of the signal, ideally suited for signal detection algorithms (such as brain-computer interfaces [31–33]).

In this setting each independent trial can be used as a trajectory for a single occupation kernel. This differs from the implementation of Koopman based DMD, where most often each snapshot corresponds to a single trajectory. The continuous time DMD method was performed using the Gaussian kernel function with  $\mu = 50$ .

Figure 2 presents the obtained eigenvalues, and Figure 3 gives log scaled spectrum obtained from the eigenvectors. It can be seen that the spectrum has strong peaks near the 12 Hz range, which suggests that the continuous time DMD procedure using occupation kernels can extract frequency information without using shifted copies of the trajectories as in [3].

For this example, the resultant dimensionality of Koopman based DMD makes the analysis of this data set intractable without discarding a significant number of samples.

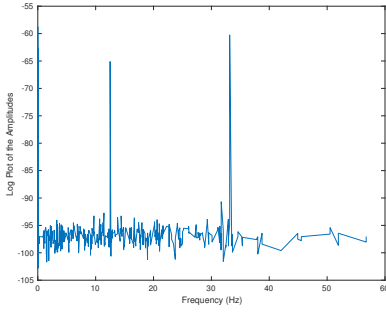


Fig. 3. Rescaled spectrum obtained from the ssVEP dataset. This doesn't quite correspond to the spectrum that would be computed through the Fourier transform. However, note the significant peak around 12 Hz, which corresponds to the ssVEP.

## V. DISCUSSION

### A. Finite Rank Representations

Since a Liouville operator is generally unbounded, convergence of the finite rank representation (in the norm topology) of Section III cannot be established for most selections of  $f$ . Note that Lemma 5 and the finite rank representation above work with the *adjoint* of the Liouville operator (i.e.,  $P_\alpha A_f^*$ ) whose domain contains the occupation kernels corresponding to the observed trajectories. As a result, to generate approximate eigenfunctions for the Liouville operator (i.e.,  $P_\alpha A_f$ ), a relationship between  $P_\alpha A_f^*$  and  $P_\alpha A_f$  must be established. Since  $P_\alpha A_f^*$  is finite-rank, it has a well-defined finite-rank adjoint  $(P_\alpha A_f^*)^*$  on  $H$  restricted to  $\text{span}(\alpha)$ , though it may not agree with  $P_\alpha A_f$  restricted to  $\text{span}(\alpha)$ , since  $\mathcal{D}(A_f)$  would have to contain  $\text{span}(\alpha)$ . If  $A_f$  is compact then  $(P_\alpha A_f^*)^*$  is equivalent to  $(P_\alpha A_f)$  when restricted to  $\text{span}(\alpha)$ . This follows since  $P_\alpha A_f^* = P_\alpha A_f^* P_\alpha$ , when restricted to  $\text{span}(\alpha)$ , and  $(P_\alpha A_f^* P_\alpha)^* = P_\alpha A_f P_\alpha = P_\alpha A_f$  on  $\text{span}(\alpha)$ . While the modally unbounded nature of  $A_f$  limits the usefulness of the above observation, it is utilized in the DMD procedure to generate a representation for  $P_\alpha A_f$ , which introduces a layer of heuristics. Since Koopman operators are also modally unbounded, they are subject to similar restrictions.

### B. Approximating the Full State Observable

The establishment the decomposition of the full state observable relies very strongly on the selection of RKHS. In the case of the Bargmann-Fock space,  $x \mapsto (x)_i$  is a function in the space for each  $i = 1, \dots, n$ . However, this is not the case for the native space of the Gaussian RBF, which does not contain any polynomials in its native space. In both cases, these spaces are universal, which means that any continuous function may be arbitrarily well estimated by a function in the space with respect to the supremum norm over a compact subset. Thus, it is not expected that a good approximation of the full state observable will hold over all of  $\mathbb{R}^n$ , but a sufficiently small estimation error is possible over a compact workspace.

### C. Scaled Liouville Operators

One advantage of the Liouville approach to DMD is that the Liouville operators may be readily modified to generate a compact operator through the so-called scaled Liouville operator (see [27]). A large class of dynamics correspond to a compact operator in this scale Liouville operator case, while Koopman operators cannot be modified in the same fashion. Allowing this compact modification, indicates that on an operator theoretic level, the study of nonlinear dynamical systems through Liouville operators allows for more flexibility in a certain sense.

The experiments presented in Section IV demonstrate that the Liouville modes obtained with the continuous time DMD procedure using Liouville operators and occupation kernels are similar in form to the Koopman modes obtained using kernel-based extended DMD [7]. Moreover, occupation kernels allow for trajectories to be utilized as a fundamental unit of data, which can reduce the dimensionality of the learning problem while retaining some fidelity that would be otherwise lost through discarding data.

## VI. CONCLUSIONS

By targeting the DMD decomposition on Liouville operators, which includes Koopman generators as a proper subset, a decomposition of a continuous time dynamical system can be performed directly rather than that of a discrete time proxy for the dynamical system with the Koopman operator. Moreover, by obviating the limiting process using the Koopman operators in the definition of Liouville operators, a broader class of dynamics is accessible through this method, since the requirement of forward completeness may be relaxed. The notion of occupation kernels were leveraged to enable a DMD analysis of the Liouville operator. Two examples were presented, one from fluid dynamics and another EEG dataset. The method presented here provides a new approach to DMD, which impacts the fundamental operator theory underlying traditional DMD with the Koopman operator.

## REFERENCES

- [1] M. Budišić, R. Mohr, and I. Mezić, "Applied koopmanism," *Chaos: An Interdisciplinary Journal of Nonlinear Science*, vol. 22, no. 4, p. 047510, 2012.
- [2] N. Črnjarić-Žic, S. Maćešić, and I. Mezić, "Koopman operator spectrum for random dynamical systems," *Journal of Nonlinear Science*, 2019.
- [3] J. N. Kutz, S. L. Brunton, B. W. Brunton, and J. L. Proctor, *Dynamic mode decomposition: Data-driven modeling of complex systems*. SIAM, 2016.
- [4] I. Mezić, "Spectral properties of dynamical systems, model reduction and decompositions," *Nonlinear Dynamics*, vol. 41, no. 1-3, pp. 309–325, 2005.
- [5] —, "Analysis of fluid flows via spectral properties of the Koopman operator," *Annual Review of Fluid Mechanics*, vol. 45, pp. 357–378, 2013.

- [6] M. O. Williams, I. G. Kevrekidis, and C. W. Rowley, "A data-driven approximation of the koopman operator: Extending dynamic mode decomposition," *Journal of Nonlinear Science*, vol. 25, no. 6, pp. 1307–1346, 2015.
- [7] M. O. Williams, C. W. Rowley, and I. G. Kevrekidis, "A kernel-based method for data-driven koopman spectral analysis," *Journal of Computational Dynamics*, vol. 2, p. 247, 2015.
- [8] A. Bittracher, P. Koltai, and O. Junge, "Pseudogenerators of spatial transfer operators," *SIAM Journal on Applied Dynamical Systems*, vol. 14, no. 3, pp. 1478–1517, 2015.
- [9] H. K. Khalil and J. W. Grizzle, *Nonlinear systems*. Prentice hall Upper Saddle River, NJ, 2002, vol. 3.
- [10] W. Haddad, *A dynamical systems theory of thermodynamics*, ser. Princeton Series in Applied Mathematics. Princeton University Press, 2019.
- [11] J. Tóth, A. L. Nagy, and D. Papp, *Reaction kinetics: Exercises, programs and theorems*. Springer, 2018.
- [12] T. G. Hallam and S. A. Levin, *Mathematical ecology: An introduction*. Springer Science & Business Media, 2012, vol. 17.
- [13] E. A. Coddington and N. Levinson, *Theory of ordinary differential equations*. Tata McGraw-Hill Education, 1955.
- [14] M. Korda and I. Mezić, "On convergence of extended dynamic mode decomposition to the Koopman operator," *Journal of Nonlinear Science*, vol. 28, no. 2, pp. 687–710, 2018.
- [15] P. Cvitanovic, R. Artuso, R. Mainieri, G. Tanner, G. Vattay, N. Whelan, and A. Wirzba, "Chaos: Classical and quantum," *ChaosBook.org (Niels Bohr Institute, Copenhagen 2005)*, vol. 69, 2005.
- [16] S. Das and D. Giannakis, "Koopman spectra in reproducing kernel Hilbert spaces," *Applied and Computational Harmonic Analysis*, 2020.
- [17] G. Froyland, C. González-Tokman, and A. Quas, "Detecting isolated spectrum of transfer and Koopman operators with fourier analytic tools," *Journal of Computational Dynamics*, vol. 1, no. 2, pp. 249–278, 2014.
- [18] D. Giannakis, "Data-driven spectral decomposition and forecasting of ergodic dynamical systems," *Applied and Computational Harmonic Analysis*, vol. 47, no. 2, pp. 338–396, 2019.
- [19] D. Giannakis and S. Das, "Extraction and prediction of coherent patterns in incompressible flows through space-time Koopman analysis," *Physica D: Nonlinear Phenomena*, vol. 402, p. 132 211, 2020.
- [20] D. Giannakis, A. Kolchinskaya, D. Krasnov, and J. Schumacher, *Koopman analysis of the long-term evolution in a turbulent convection cell*, arXiv:1804.01944, 2018.
- [21] J. A. Rosenfeld, B. Russo, R. Kamalapurkar, and T. T. Johnson, *The occupation kernel method for nonlinear system identification*, arXiv:1909.11792, 2019.
- [22] J. A. Rosenfeld, R. Kamalapurkar, B. Russo, and T. T. Johnson, "Occupation kernels and densely defined Liouville operators for system identification," in *IEEE Conference on Decision and Control*, IEEE, 2019, pp. 6455–6460.
- [23] G. K. Pedersen, *Analysis now*. Springer Science & Business Media, 2012, vol. 118.
- [24] M. T. Jury, "C\*-algebras generated by groups of composition operators," *Indiana University Mathematics Journal*, pp. 3171–3192, 2007.
- [25] K. E. Luery, *Composition operators on hardy spaces of the disk and half-plane*. University of Florida, 2013.
- [26] I. Steinwart and A. Christmann, *Support vector machines*. Springer Science & Business Media, 2008.
- [27] J. A. Rosenfeld, R. Kamalapurkar, L. F. Gruss, and T. T. Johnson, *Dynamic mode decomposition for continuous time systems with the Liouville operator*, arXiv:1910.03977, 2019.
- [28] L. F. Gruss and A. Keil, "Sympathetic responding to unconditioned stimuli predicts subsequent threat expectancy, orienting, and visuocortical bias in human aversive pavlovian conditioning," *Biological psychology*, vol. 140, pp. 64–74, 2019.
- [29] D. Regan, "Human brain electrophysiology," *Evoked potentials and evoked magnetic fields in science and medicine*, 1989.
- [30] N. M. Petro, L. F. Gruss, S. Yin, H. Huang, V. Miskovic, M. Ding, and A. Keil, "Multimodal imaging evidence for a frontoparietal modulation of visual cortex during the selective processing of conditioned threat," *Journal of cognitive neuroscience*, vol. 29, no. 6, pp. 953–967, 2017.
- [31] H. Bakardjian, T. Tanaka, and A. Cichocki, "Optimization of SSVEP brain responses with application to eight-command brain-computer interface," *Neuroscience letters*, vol. 469, no. 1, pp. 34–38, 2010.
- [32] G. Bin, X. Gao, Z. Yan, B. Hong, and S. Gao, "An online multi-channel SSVEP-based brain-computer interface using a canonical correlation analysis method," *Journal of neural engineering*, vol. 6, no. 4, p. 046 002, 2009.
- [33] M. Middendorf, G. McMillan, G. Calhoun, and K. S. Jones, "Brain-computer interfaces based on the steady-state visual-evoked response," *IEEE transactions on rehabilitation engineering*, vol. 8, no. 2, pp. 211–214, 2000.